Available online at www.sciencedirect.com
SCIENCE DIRECT®
ELSEVIER
Nuclear Instruments and Methods in Physics Research B 230 (2005) 330–339
NIM B
Beam Interactions with Materials & Atoms
www.elsevier.com/locate/nimb

High negative ion yield from light molecule scattering

J.A. Scheer [a,*], M. Wieser [a], P. Wurz [a], P. Bochsler [a], E. Hertzberg [b], S.A. Fuselier [b], F.A. Koeck [c], R.J. Nemanich [c], M. Schleberger [d]

[a] *Physikalisches Institut, University of Bern, Sidlerstrasse 5, 3012 Bern, Switzerland*
[b] *Lockheed Martin, Advanced Technology Center, 3251 Hanover St., Palo Alto, CA 94304, USA*
[c] *Department of Physics, North Carolina State University, Raleigh, NC 27695-8202, USA*
[d] *Institut für Experimentelle Physik, Universität Duisburg-Essen, Universitätsstraße 5, 45117 Essen, Germany*

Abstract

Molecular oxygen and hydrogen ions were scattered at grazing incidence from several diamond-like carbon (DLC) surfaces in the energy range from 190 eV to 2400 eV. Most surfaces were hydrogen terminated. For incident positive oxygen ions, scattered negative ion fractions of up to 33% were recorded, and for incident positive hydrogen ions, negative ion fractions of more than 5% were measured. These values are among the highest ever reported, especially for oxygen. They have been matched only by results of scattering experiments using a hydrogen terminated surface of natural diamond.

Keywords: Diamond like carbon (DLC); Neutral particle imaging; Particle scattering; Surface ionization; Tetrahedral amorphous carbon; ta-C

1. Introduction

Interaction of atomic and molecular projectiles with insulating surfaces has gained considerable attention in recent years [1–9]. Reports of relatively high fractions of negative ions resulting from scattering of positive atomic and molecular ions off insulating surfaces were quite unexpected, but suggested possibilities for several new applications. Among these applications we propose to use this process for efficient detection of 5 eV to 2 keV neutral particles in interplanetary and interstellar space [10,12,13]. The proof of concept for this detection technique has already been demonstrated in space. The mass spectrograph on the IMAGE satellite mission, designed to detect low energy neutral atoms, uses a conversion surface of volatile adsorbates on a polished, poly-crystalline W substrate to convert a fraction of incoming neutral atoms to negatively charged ions [11,14].

* Corresponding author. Fax: +41 31 631 4405.
E-mail address: jscheer@phim.unibe.ch (J.A. Scheer).

0168-583X/$ - see front matter © 2004 Elsevier B.V. All rights reserved.
doi:10.1016/j.nimb.2004.12.063

For future missions, including interplanetary missions, a conversion surface with better controlled long-term stability and higher yield is desired. A natural diamond surface has been demonstrated to be an excellent candidate for such purposes [1,15,16], but it comes with the disadvantages of limited availability and extremely high price.

Since interstellar gas is expected to consist mainly of H and He with traces of O, N, C and Ne [17] and a diamond surface has already demonstrated high yield, we tested diamond-like carbon surfaces using H and O molecules. In these tests, positive molecular oxygen and hydrogen ions were scattered off tetrahedral amorphous carbon (ta-C; a subset of DLC) surfaces with and without hydrogen termination. Molecular ions were used because they can be produced far more efficiently than atomic ions in our systems. The impact of using positively charged molecular ions on the results is discussed in detail below. The following results from these tests are presented here:

- ionization efficiencies for negative ion production and
- scattering properties, i.e. angular scattering distributions of the scattered beam.

The measurements were done at moderate vacuum conditions, i.e. in the low 10^{-7} mbar range, which mirror the conditions within a typical particle sensing satellite instrument shortly after launch. From the European Space Agency (ESA) ROSETTA mission it is known that several weeks after launch, pressure in the vicinity of the spacecraft drops to the low 10^{-9} mbar range, and into the 10^{-10} mbar range after few months. Pressure inside space instruments with small external openings, such as most particle instruments, are expected to be at least an order of magnitude higher than the pressures surrounding the spacecraft. Adding internal outgassing, pressures in the 10^{-8} mbar range are expected to persist in future space particle instruments more or less indefinitely. Furthermore, additional measurements were done at ultra-high vacuum (UHV) conditions with another apparatus (base pressure in the low 10^{-10} mbar range) to ensure that the observed effects were not induced by adsorbates.

Hydrogen termination is an important issue for these tests. There are two reasons the measurements reported here have been made mostly with hydrogen terminated surfaces. Firstly, from previous measurements it is known that hydrogen termination of a pure diamond surface increases its yield of negative ions significantly [1]. This is explained by a change of the surface electronic structure when hydrogen terminated from positive electron affinity (PEA) [18] to negative electron affinity (NEA) [19,20], making more electrons available for the electron transfer process. Secondly, the DLC surfaces used here are tetrahedral amorphous carbon (ta-C) thin films with a high fourfold content (fraction of C displaying sp^3 bonding). At the surface, each carbon atom is bonded to only three other carbon atoms leaving one free bond, theoretically orientated perpendicular to the surface and called a dangling bond [18,21,22]. These bonds are very reactive to adsorbates. H termination saturates dangling bonds with hydrogen atoms, and the resultant C–H bonds are even stronger and more inert than the C–C bonds at the surface, providing the advantage of a tough and durable surface where needed, as in the harsh sputtering environment of space. This is particularly desirable for space applications where decontamination of conversion surfaces at elevated temperatures during the mission is not feasible for power and thermal reasons.

A comparable effect has been observed in friction experiments on hydrogen free and hydrogen terminated DLC films [32]. When surfaces are well cleaned, the coefficient of friction of hydrogen-terminated films is two orders of magnitude lower than that of hydrogen free films. With the introduction of humidity, the friction coefficients of hydrogen free films drop while those for hydrogen terminated surfaces rise, leaving only one order of magnitude between them. This is consistent with the presence of adsorbates, primarily water, on the hydrogen free surface. These adsorbates saturate the free C bonds, resulting in a smoother surface. With hydrogen termination, the presence of adsorbates results in greater surface roughness. Still, the coefficient of friction of the hydrated hydrogen terminated surface remains an order of

magnitude lower that the hydrated hydrogen free surface, indicating a reduced adsorbate load.

2. Experiment

The Si wafers used as substrates for the ta-C films are 1 mm thick with the ⟨1 0 0⟩ face exposed, and boron doped for conductivity in the 1–20 Ω cm range. Cut and polished wafer surfaces were measured to be within 0.13° of the actual ⟨1 0 0⟩ lattice plane. Tetrahedral amorphous-carbon (ta-C) thin films were prepared by pulsed laser deposition (PLD) using an excimer laser (248 nm, Lambda Physik Compex® 150 configured in the power oscillator power amplifier mode) at high fluence (~100 J/cm^2) to ablate a pyrolytic graphite target in vacuum ($<1\times10^{-6}$ mbar). Under these conditions the ablated carbon flux is highly ionized with a broad energy distribution ranging from 20 eV to 300 eV. The carbon ions penetrate and implant in the near surface region (called subplantation [25]) causing densification and buildup of stress, ultimately leading to high fourfold (i.e. sp^3) content measured at >80% [26] of the amorphous films. The subplantation also suppresses surface diffusion, which is thought to be one reason why these films are so smooth. Electrical conductivity [27,28] depends sensitively on the amount of threefold (i.e. sp^2) coordinated carbon present, and the degree of clustering and/or chain formation. The electron conduction is accomplished by hopping from threefold clusters mediated by the cluster size and spacing. Typically, resistivities of 10^6 Ω cm are found for high fourfold content films, but resistivities have been measured down to 10 Ω cm in annealed films with slightly lower fourfold content. The hydrogen termination process, when applied, occurs at approximately 450 °C in 27 mbar of pure hydrogen, with 700 W of microwave power applied for 60 s. It is important to note the importance of surface smoothness in minimizing scattering losses in the downstream particle collection and analysis system of any test apparatus or instrument. The exceptional smoothness of these ta-C samples, approaching perfect smoothness (<1 Å rms) when processed optimally, was an important criterion in selecting this material. An overview of the properties of the different surfaces is given in Table 1.

Measurements were made in part at the University of Bern, Switzerland, and in part at the University of Duisburg-Essen, Germany. The two setups will be described briefly. More detail on both experimental setups can be found in [10,23] and [24], respectively. The experiment ILENA at the University of Bern consists of an ion source, a beam-filter and -guiding system, a sample stage with housing and a detection unit. All these units are contained in a single vacuum chamber pumped by an iongetter pump. For the measurements reported here an impact angle of 8° with respect to the surface plane has been chosen. The reflected beam is recorded using a two-dimensional position-sensitive MCP detector with a viewing angle of ±12.5° in both azimuthal and polar direction. A retarding potential analyzer (RPA) consisting of three grids is mounted in front of the MCP detector. The detector unit, including the RPA, is shielded electrostatically and can be rotated independently from the converter surface around the same axis. The outer grids of the RPA are

Table 1
Surface properties of the samples tested in this study are tabulated

Film material	Film thickness [Å]	Surface roughness [Å rms]	Hydrogen termination	Substrate
ta-C	181	4.5	Yes	Si
ta-C	78	5	Yes	Si
ta-C	1050	3	Yes	Si
ta-C	1075	0.7	Yes	Si
ta-C	1075	1	No	Si
–	–	20–30	Yes	Amorph C

Note that there is only one sample without H termination and that one sample is not a ta-C coated surface, but purely amorphous carbon.

grounded to shield the inner grid, which can be biased to suppress positive ions. An additional grid in front of the MCP detector at negative potential with respect to the MCP detector serves to reject secondary electrons originating from the preceding grids and the converter surface. The MCP detector may be floated to a high negative voltage with respect to the converter surface in order to vary the transmission threshold for negative particles. After baking out the vacuum chamber at 80 °C for several hours, a residual gas pressure of 5×10^{-8} mbar is achieved. During operation the pressure may rise into the low 10^{-7} mbar range as a result of test gas leaking into the ion source chamber.

The experimental system JUSO [23,24] (recently moved from the University of Osnabrück to the University of Duisburg-Essen) is a UHV system with an achievable base pressure of 3×10^{-10} mbar. For the measurements reported here the base pressure was 1×10^{-9} mbar and remained in the low 10^{-9} mbar range during the measurements. Ions are extracted from an ion plasma source and are mass analyzed by a 90° sector field magnet. Using an electric deflection system in front of the analyzing magnet, the primary beam can be pulsed to allow time-of-flight (TOF) measurements. The scattering surface is mounted onto a three-axis manipulator equipped with thermocouple-controlled electron beam heating. Downstream from the scattering surface, a collimating tube providing 1.2° full field of view and a microsphere plate (MSP) detector are mounted under a fixed scattering angle of 10° with respect to the incident beam. The angle of incidence is fixed at 5° from the surface plane to assure specular scattering conditions. After the scattering surface a post-acceleration voltage can be applied to separate ions from neutrals. For reasons mentioned above, the measurements at JUSO have been made with a hydrogen terminated DLC surface. The sample was heated to 600 °C, which may have slightly decreased the smoothness after removing most of the adsorbates [29]. The hydrogen termination remained unaffected since thermal desorption of hydrogen does not occur below 700 °C [30]. Target cleanliness was verified continually by the TOF technique (looking for recoil ions) throughout all JUSO tests. Negative charge state fractions were measured at both facilities. Angular scattering distributions were measured only in the ILENA, and energy distributions only in the JUSO apparatus.

3. Results and discussion

Although we eventually want to use neutral atoms to study surface ionization, for these experiments we used positive molecular ions because they can be produced far more efficiently, and with much better energy, intensity and angle control in our systems than can neutrals. In the following the consequences will be discussed.

From previous experiments with a polycrystalline diamond surface [10] and a diamond single-crystal surface [1,15], it was established that incident hydrogen and oxygen ions are effectively neutralized while scattering off diamond-like surfaces. This is supported by the fact that we did find very low positive charge state fractions for oxygen (below 1%) and hydrogen (several percent) with the measurements reported here, indicating effective neutralization upon scattering. Furthermore, these values are in good agreement with results for scattering experiments using an MgO crystal [12] (which, like diamond, is an insulator, but has an even wider bandgap) where both neutrals and ions were used as incident particles. As a result, we can assume complete memory loss of the incident charge state after scattering.

For the use of molecules instead of atoms, the situation is different. A molecule has many more electronic states than an atom, so we cannot expect the charge exchange process while scattering to be identical. But according to Wurz et al. [10], more than 80% of molecules with energy in the 300–800 eV range, when scattered off a polycrystalline diamond surface, dissociate just before reaching the surface, on the incoming stage of the trajectory. That means that final charge state fraction is determined mainly by charge exchange processes between the surface and dissociated atoms. Analysis of the JUSO spectra (energy range: 850–2500 eV) revealed molecular survival fractions of about 10% for both hydrogen and oxygen,

decreasing with increasing energy, which fits well with those data. Therefore, we conclude that use of molecules causes a negligible change to the charge state fractions measured in this study.

3.1. ILENA measurements

Table 1 lists structural properties of the examined surfaces. The hydrogen terminated surfaces are of three of film thicknesses (<100 Å, ~200 Å, ~1000 Å), and though they are all tetrahedral amorphous-carbon (ta-C) surfaces, they were supplied by three different manufacturers and could have had somewhat different scattering properties. Furthermore, for comparison reasons there is one surface of solid amorphous carbon, rather than a film, and one ta-C surface without hydrogen termination. All these surfaces were made by standard processes [31] for assurance of consistently reproducible properties. This is important because the conversion surface area needed for typical, neutral particle sensing space instruments may reach 500 cm^2. The two key requirements for successful conversion surface performance are high ionization yield and low angle scattering, the latter to minimize scattered particle loss in downstream detection systems. The component of angle deviation from specular scattering that resides in a plane containing the incoming trajectory and normal to the surface is defined as polar scattering, with zero indicating a true specular reflection. The component of specular scattering normal to the polar angle plane is defined as azimuthal scattering. Fig. 1 shows an example of an angular scattering distribution measured with the ILENA apparatus. Here FWHM azimuthal and polar scattering angles are 18° and 10°, respectively. For all surfaces the measured FWHM scattering angles resulting from incident hydrogen and oxygen molecular ions with various incident energies are shown in Figs. 2 and 3, respectively. The general trend is toward increased angular scattering with increasing incident energy. Moreover, angular scattering in the polar direction is about a factor of two smaller than in the azimuthal direction. The four hydrogen terminated ta-C surfaces display similar measured performance, and the ta-C surface without hydrogen termination performs almost as well, with the exception that at the lowest incident energies the scattering is worse. No explanation has yet been determined for this behaviour at low energies. Note that for natural diamond the best performance was also achieved with H termination [1]. The amorphous carbon surface shows significantly worse scattering than other samples, which is consistent with its higher surface roughness, as listed in Table 1. Therefore, amorphous carbon is not a recommended conversion surface candidate at

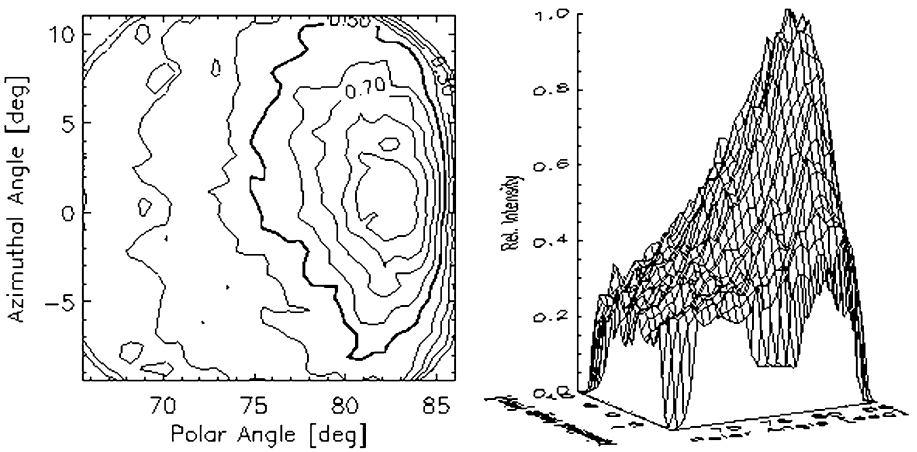

Fig. 1. Angular scattering distribution of O^- ions resulting from 390 eV O_2^+ incident on a hydrogen terminated ta-C surface with a film thickness of 1050 Å. FWHM angular scattering widths in the azimuthal and polar directions are 18° and 10°, respectively. Measurements were taken using the ILENA apparatus.

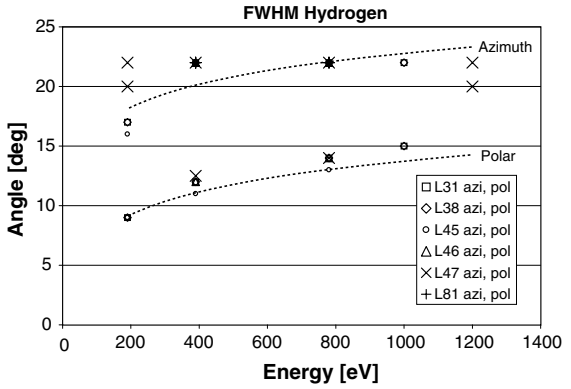

Fig. 2. Energy dependence of H^- angular scattering resulting from incident H_2^+. The data are presented in pairs showing FWHM in the azimuthal and polar directions for each surface. The dashed lines are to guide the eye. Measurements were taken using the ILENA apparatus.

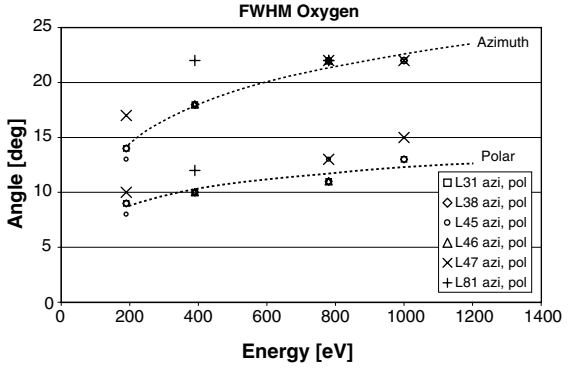

Fig. 3. Energy dependence of O^- angular scattering resulting from incident O_2^+. The data are presented in pairs showing FWHM in the azimuthal and polar directions for each surface. The dashed lines are to guide the eye. Measurements were taken using the ILENA apparatus.

this time. If polishing techniques for amorphous carbon can be improved sufficiently in the future, this surface should be reconsidered.

Negative charge state fractions, i.e. ionization efficiencies, of all six samples tested are displayed in Fig. 4. With the detection system of the ILENA apparatus we cannot distinguish between atomic and molecular ions, but, as mentioned above, the fraction of molecular ions is very low and will thus not have a big influence on the results. Amorphous carbon shows good ionization efficiency, especially

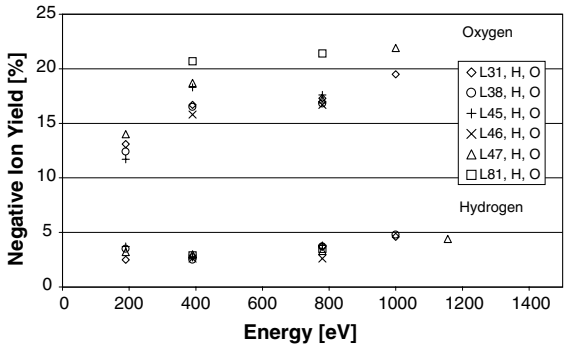

Fig. 4. Negative charge state fractions resulting from incident O_2^+ and H_2^+. Values higher than 10% represent oxygen ions; values below 10% represent hydrogen ions. The errors are ±1% for hydrogen ions and ±2% for oxygen ions. Measurements were taken using the ILENA apparatus only.

for oxygen. For the other surfaces, ionization efficiencies are comparable. Within the energy range investigated (190–1200 eV) ionization efficiency increases with increasing incident energy. Using hydrogen molecules as incident ions, ionization efficiencies vary between 2.5% and 5%, and using oxygen molecules they vary between 11% and 22%. These efficiencies are slightly higher than those reported from measurements with other insulating surfaces like MgO [12] and $BaZrO_3$ [23]. However no benefit appeared in ionization efficiencies due to hydrogen termination. This is most likely caused by the moderate vacuum conditions in the ILENA apparatus ($\approx 1 \times 10^{-7}$ mbar), which result in continuous adsorbate recontamination of the surface by residual gas.

3.2. JUSO measurements

For measurements under UHV conditions, a hydrogen terminated ta-C surface was chosen with a film thickness of 1050 Å. A typical energy spectrum, where time-of-flight (TOF) is converted into particle energy, is shown in Fig. 5, using incident O_2^+ with an incident energy of 1801 eV. The large lower energy peak is the sum of the neutral atoms produced by dissociation and of the surviving neutral molecules. The molecules form a narrow peak on top of the broad distribution of the dissociated atoms. Because of successive collisional energy

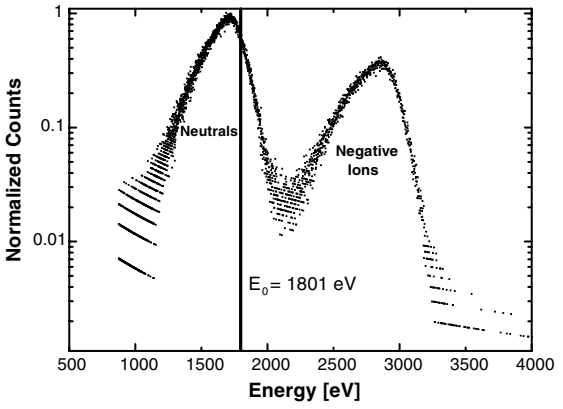

Fig. 5. Time-of-flight (TOF) spectra, in which time has been converted to particle energy and normalized. Due to the applied positive postacceleration voltage, the ion distribution is shifted to the right of the neutral distribution. The vertical line represents the nearly monoenergetic incident beam, before scattering, with primary energy E_0. The spectra shows relative O and O^- fractions resulting from 1801 eV O_2^+ scattered off a hydrogen terminated ta-C surface with a film thickness of 1050 Å. Measurements were taken using the JUSO apparatus.

losses, called straggling, in the scattering process, the scattered neutral particle distribution falls mostly below the incident particle energy. This distribution exceeds partly the incident particle energy because of the energy gain of the atoms in the dissociation process. This gain is "multiplied" when converting from the centre of mass system, where the dissociation actually happens, to the laboratory system, where the process is observed, according to:

$$E = \tfrac{1}{2}E_0 + \tfrac{1}{2}E_D \pm \sqrt{E_0 \cdot E_D \cdot \cos\alpha}.$$

Here E_0 is incident particle energy, E_D is dissociation energy and α is the angle between the molecular axis and the incident beam direction. The higher energy peak shows the displaced distribution of negative oxygen ions. Separation is accomplished by a post-acceleration voltage that shifts the ion peak to the right.

In order to complete analysis of the charge state fractions it was necessary to quantify the energy spectra and to include corrections for detector efficiency losses. The former was accomplished by use of an asymmetrical exponential fitting function as described in [9]. The detection efficiency (i.e. the probability that the detector will sense an incoming particle) of the ILENA MCP assembly had long been established, but that for the JUSO apparatus turned out to be too difficult to measure unambiguously in time for inclusion in this report. Fig. 6 depicts negative charge state fractions, i.e. ionization efficiencies, for the entire energy range of 190–2500 eV, calculated using combined ILENA and JUSO data with detection efficiency corrections included in the ILENA data, but not those from the JUSO apparatus, as stated above. Note that the measurements were done at different vacuum conditions. During operation the pressures were in the low 10^{-7} mbar and 10^{-9} mbar range at ILENA and JUSO, respectively. While for the ILENA measurements we cannot exclude effects induced by the presence of adsorbates, at JUSO particles were scattered off a definitely clean surface, controlled by continuous search for recoil atoms. Lower negative charge state fractions measured with JUSO (compared to ILENA) would thus mean that data taken with ILENA were affected by surface contamination. From Fig. 6 we see that this is not the case.

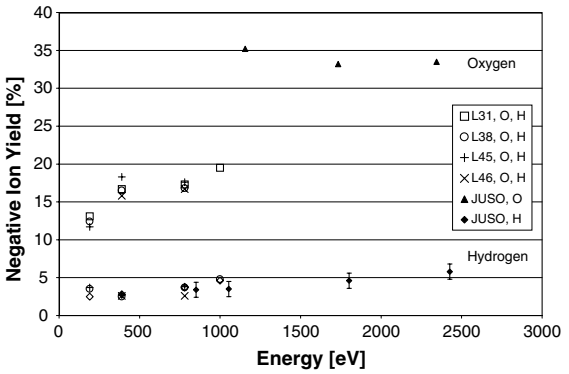

Fig. 6. Negative charge state fractions resulting from incident O_2^+ and H_2^+ scattered off hydrogen terminated ta-C surfaces, as measured in both ILENA (incident energy 190–1200 eV, open symbols and crosses) and JUSO systems (incident energy 850–2500 eV, closed symbols) combined. As in Fig. 4, values higher than 10% represent oxygen ions. The JUSO data have not yet been corrected for detection efficiency in the MSP detector, which affects mainly the values for oxygen ions at 1150 eV and 1700 eV, resulting in overstated charge state fractions. See text for details.

3.2.1. Hydrogen

The detection efficiency for hydrogen in the energy range from 190 eV to 2400 eV has been found to be at least 70%, but is probably closer to 100% [33,34]. This uncertainty is indicated by error bars in Fig. 6, and within these error bars the agreement of measurements from ILENA and JUSO is excellent. Taking into account the difference in vacuum conditions between ILENA and JUSO, this similarity supports the thesis that hydrogen terminated surfaces strongly displace adsorbates. Overall, the negative charge state fraction increases with increasing incident particle energy from about 2.5% to 5%.

3.2.2. Oxygen

Our measurements demonstrated that the detection efficiency of oxygen with an incident energy of 2400 eV is very close to 100% but drops significantly with decreasing incident energy. More precise information about this decrease is not yet available. The high negative charge state fractions (>30%) at 1150 eV and 1700 eV incident energy in Fig. 6 are therefore overstated. However, the high negative charge state fraction of 33% at 2400 eV incident energy fits well with negative charge state fractions measured while scattering off a hydrogen terminated surface of a super-polished, natural diamond [1]. At lower energies the negative charge state fraction is expected to drop more or less linearly to the values measured with ILENA.

Finally, the question remains how charge exchange happens while positive ions scatter off an insulating surface. The valence band of diamond has a bandwidth of 21 eV, and the width of the bandgap is 5.47 eV. The hydrogen-terminated diamond surface exhibits a negative electron affinity of 0.7 eV, i.e. the bottom of the conduction band is above the vacuum level by approximately 0.7 eV. The affinity levels of H and O are 0.754 eV and 1.462 eV, respectively, below the vacuum level. The valence band is formed by the sp^3 hybridised C electrons, the bonds are absolutely covalent. The valence band is filled and there is no electron mobility. So all models using the conventional idea of resonant electron capture from the conduction band (as for metals) can be excluded from further discussion. It is important to mention that although the surfaces tested here are diamond-like carbon surfaces, their high sp^3 content (~80%) allows us to apply the same discussion as for natural diamond.

For ionic crystals (e.g. LiF) charge exchange proceeds via capture of electrons from the anionic sites of the surface [35–37] in a binary ion-atom interaction. Once the negative ion is formed it cannot be destroyed by resonant electron loss (as in the case of metals) because of the bandgap of the ionic crystal. Diamond is no ionic crystal, there is no such charge localization, but the latter conclusion applies to diamond as well. When an ion approaches a surface, due to the image potential its affinity level experiences a downward shift. In contrast to ionic crystals, below a certain surface-ion distance charge transfer could be possible because of the smaller bandgap of diamond. Furthermore, the probability for a particle to be negatively charged increases with increasing effective number of collisions, and thus at grazing incidence angles.

Maazouz et al. [38–40] reported results of O^- and H^- fractions while scattering off Al, a jellium type metal, and off Si, a semiconductor with a bandgap of 1.1 eV. Surprisingly, despite the differences in electronic structures they found comparable ion fractions for both surfaces. The authors suggested, taking parallel velocity effects and dangling bonds into account, the presence of surface states at the Si surface to be responsible for their findings.

A theoretical approach is given by Lorente et al. [41]. Calculations for H^- formation while scattering off Al, Si and LiF showed comparable electron hopping probabilities for Al and Si. Furthermore, the parallel velocity of the projectile caused a smoothening of the surface density of states, SDOS, of Si to make it look like Al for the moving particle.

We safely extend these arguments to diamond being very similar to Si. The observed higher fractions of negative ions in the case of diamond as the scattering surface are then explained by the larger bandgap of diamond, which hinders electron loss on the outgoing trajectory. However, additional work is still necessary to fully understand negative ion formation while scattering off insulating surfaces.

4. Conclusions

High fractions of negative ions, 12–33% for oxygen and 2.5–5% for hydrogen, have been measured as a result of scattering incident O_2^+ and H_2^+ with initial energies of 190–2400 eV off several diamond-like carbon (ta-C) surfaces. Compared to previous measurements with other surfaces these ionization efficiencies are among the highest ever reported [1,12,23,24]. With the moderate vacuum conditions at the ILENA apparatus (1×10^{-7} mbar) the benefits of hydrogen termination on ionization efficiency and scattering were obscured. Scattering experiments using a hydrogen terminated diamond-like carbon surface with controlled surface cleanness at the JUSO apparatus showed similar negative charge state fractions compared to previous measurements with a hydrogen-terminated natural diamond surface [1]. These previous measurements were done with hydrogen-terminated and hydrogen free surfaces, where increase of the negative charge state fraction due to hydrogen-termination was clearly demonstrated. So it is safe to conclude, that the very high negative charge state fractions found from hydrogen-terminated diamond-like carbon surfaces are also related to hydrogen-termination.

Furthermore, the match of the data taken under different vacuum conditions supports the thesis that hydrogen terminated surfaces strongly displace adsorbates. This is also supported by the fact that angular scattering spread from all tested ta-C surfaces was minimal. As a result, these surfaces are strong candidates for space borne neutral particle conversion. Finally, ta-C films applied to highly polished silicon wafers are readily available, are affordable in large areas and provide consistently reliable results, all of which are of great importance for today's and future applications in space research.

Acknowledgements

This work is supported by the Swiss National Science Foundation. The authors are grateful to Dr. T.A. Friedmann at Sandia National Laboratories, for preparation of the ta-C samples.

References

[1] J.A. Scheer, Master Thesis, University of Osnabrück, Germany, 1999.
[2] C. Auth, A.G. Borisov, H. Winter, Phys. Rev. Lett. 75 (1995) 2292.
[3] P. Stracke, F. Wiegershaus, S. Krischok, H. Müller, V. Kempter, Nucl. Instr. and Meth. B 125 (1997) 63.
[4] S.A. Deutscher, A.G. Borisov, V. Sidis, Phys. Rev. A 59 (1999) 4446.
[5] P. Roncin, J. Villette, J.P. Atanas, H. Khemliche, Phys. Rev. Lett. 83 (1999) 864.
[6] A.G. Borisov, V.A. Esaulov, J. Phys. Condens. Matter 12 (2000) R177.
[7] R. Souda, Int. J. Mod. Phys. B 14 (2000) 1139.
[8] H. Winter, Phy. Rep. 367 (2002) 387.
[9] J.A. Scheer, P. Wurz, W. Heiland, Nucl. Instr. and Meth. B 212 (2003) 291.
[10] P. Wurz, R. Schletti, M.R. Aellig, Surf. Sci. 373 (1997) 56.
[11] P. Wurz, M.R. Aellig, P. Bochsler, A.G. Ghielmetti, E.G. Shelley, S. Fuselier, F. Herrero, M.F. Smith, T. Stephen, Opt. Eng. 34 (1995) 2365.
[12] M. Wieser, P. Wurz, K. Brüning, W. Heiland, Nucl. Instr. and Meth. B 192 (2002) 370.
[13] P. Wurz, in: The Outer Heliosphere: Beyond the Planets, Copernikus Gesellschaft e.V., Katlenburg-Lindau, 2000, p. 251.
[14] T.E. Moore, D.J. Chornay, M.R. Collier, F.A. Herrero, J. Johnson, M.A. Johnson, J.W. Keller, J.F. Laudadio, J.F. Lobell, K.W. Ogilvie, P. Rozmarynowski, S.A. Fuselier, A.G. Ghielmetti, E. Hertzberg, D.C. Hamilton, R. Lundgren, P. Wilson, P. Walpole, T.M. Stephen, B.L. Peko, B. van Zyl, P. Wurz, J.M. Quinn, G.R. Wilson, Space Sci. Rev. 91 (2000) 155.
[15] J.A. Scheer, K. Brüning, T. Fröhlich, P. Wurz, W. Heiland, Nucl. Instr. and Meth. B 157 (1999) 208.
[16] P. Wurz, T. Fröhlich, K. Brüning, J.A. Scheer, W. Heiland, E. Hertzberg, S. Fuselier, in: J. Safrankov, A. Kanka (Eds.), Prague Proceeding Week of Postdoc. Students, 1998, p. 257.
[17] J. Geiss, M. Witte, Space Sci. Rev. 78 (1996) 229.
[18] B.B. Pate, Surf. Sci. 165 (1986) 83.
[19] F.J. Himpsel, J.A. Knapp, J.A. van Vechten, D.E. Eastman, Phys. Rev. B 20 (1979) 624.
[20] C. Bandis, B.B. Pate, Surf. Sci. 350 (1996) 315.
[21] S. Evans, in: J. Field (Ed.), The Properties of Natural and Synthetic Diamond, Academic Press, 1992.
[22] G. Kern, J. Hafner, G. Kresse, Surf. Sci. 366 (1996) 445.
[23] S. Jans, P. Wurz, R. Schletti, K. Brüning, K. Sekar, W. Heiland, J. Quinn, R.E. Leuchter, Nucl. Instr. and Meth. B 173 (2001) 503.
[24] B. Willerding, H. Steininger, K.J. Snowdon, W. Heiland, Nucl. Instr. and Meth. B 2 (1984) 453.
[25] Y. Lifshitz, S.R. Kasi, J.W. Rabalais, Phys. Rev. Lett. 62 (1989) 1290.
[26] T.M. Alam, T.A. Friedmann, P.A. Schultz, D. Sebastiani, Phys. Rev. B 67 (2003) 245309.

[27] J.P. Sullivan, T.A. Friedmann, in: Proc. of the 1st International Specialist Meeting on Amorphous Carbon, World Scientific Publ., Singapore, 1998.
[28] J.P. Sullivan, T.A. Friedmann, R.G. Dunn, E.B. Stechel, P.A. Schultz, N. Missert, Mat. Res. Soc. Proc. 498 (1998) 97.
[29] X.L. Peng, Z.H. Barber, T.W. Clyne, Surf. Coat. Technol. 138 (2001) 23.
[30] C. Su, J.C. Lin, Surf. Sci. 406 (1998) 149.
[31] T.A. Friedmann, Personal communication, Sandia National Laboratories.
[32] A. Erdemir, Surf. Coat. Technol. 146–147 (2001) 292.
[33] S. Jans, Master Thesis, University of Bern, Switzerland, 1999.
[34] S. Jans, P. Wurz, R. Schletti, T. Fröhlich, E. Hertzberg, S. Fuselier, J. Appl. Phys. 87 (2000) 2587.
[35] C. Auth, A. Mertens, H. Winter, A.G. Borisov, V. Sidis, Phys. Rev. A 57 (1998) 351.
[36] F.W. Meyer, Q. Yan, P. Zeijlmans van Emmichoven, I.G. Hughes, G. Spierings, Nucl. Instr. and Meth. B 125 (1997) 138.
[37] S. Ustaze, R. Verrucchi, S. Lacombe, L. Guillemot, V.A. Esaulov, Phys. Rev. Lett. 79 (1997) 3526.
[38] M. Maazouz, R. Baragiola, A. Borisov, V.A. Esaulov, J.P. Gauyacq, L. Guillemot, S. Lacombe, D. Teillet-Billy, Surf. Sci. 364 (1996) 568.
[39] M. Maazouz, L. Guillemot, T. Schlathölter, V.A. Esaulov, Nucl. Instr. and Meth. B 125 (1997) 283.
[40] M. Maazouz, S. Ustaze, L. Guillemot, V.A. Esaulov, Surf. Sci. 409 (1998) 189.
[41] N. Lorente, J. Merino, F. Flores, M.Yu. Gusev, Nucl. Instr. and Meth. B 125 (1997) 277.